



Missouri University of Science and Technology
Scholars' Mine

International Specialty Conference on Cold-Formed Steel Structures

(2012) - 21st International Specialty Conference on Cold-Formed Steel Structures

Aug 24th, 12:00 AM - Aug 25th, 12:00 AM

Finite Element Analyses of Lipped Chanel Beams with Web Openings in Shear

P. Keerthan

M. Mahendran

Follow this and additional works at: <https://scholarsmine.mst.edu/isccss>

 Part of the [Structural Engineering Commons](#)

Recommended Citation

Keerthan, P. and Mahendran, M., "Finite Element Analyses of Lipped Chanel Beams with Web Openings in Shear" (2012). *International Specialty Conference on Cold-Formed Steel Structures*. 4.
<https://scholarsmine.mst.edu/isccss/21iccfss/21iccfss-session4/4>

This Article - Conference proceedings is brought to you for free and open access by Scholars' Mine. It has been accepted for inclusion in International Specialty Conference on Cold-Formed Steel Structures by an authorized administrator of Scholars' Mine. This work is protected by U. S. Copyright Law. Unauthorized use including reproduction for redistribution requires the permission of the copyright holder. For more information, please contact scholarsmine@mst.edu.

Finite Element Analyses of Lipped Channel Beams with Web Openings in Shear

P. Keerthan¹ and M. Mahendran²

Abstract

Cold-formed steel members are increasingly used as primary structural elements in buildings due to the availability of thin and high strength steels and advanced cold-forming technologies. Cold-formed lipped channel beams (LCB) are commonly used as flexural members such as floor joists and bearers. Shear behaviour of LCBs with web openings is more complicated and their shear capacities are considerably reduced by the presence of web openings. However, limited research has been undertaken on the shear behaviour and strength of LCBs with web openings. Hence a numerical study was undertaken to investigate the shear behaviour and strength of LCBs with web openings. Finite element models of simply supported LCBs with aspect ratios of 1.0 and 1.5 were considered under a mid-span load. They were then validated by comparing their results with test results and used in a detailed parametric study. Experimental and numerical results showed that the current design rules in cold-formed steel structures design codes are very conservative for the shear design of LCBs with web openings. Improved design equations were therefore proposed for the shear strength of LCBs with web openings. This paper presents the details of this numerical study of LCBs with web openings, and the results.

Keywords: *Lipped Channel beams, Web openings, Shear capacity, Cold-formed steel structures, Finite element analyses.*

1. Introduction

Cold-formed steel sections are frequently used in residential, commercial and industrial buildings (Figure 1). The cold-formed steel structural members such as the 'C', 'Z' or tubular sections are commonly used in floor and roofing frame

¹ Post-doctoral Research Associate and ²Professor, Science and Engineering Faculty, QUT, Australia.

systems, wall elements, and structural members for trusses and many other load bearing systems. The increasing use of cold-formed steel sections has enhanced interest in the design and efficiency of cold-formed steel members. Among them, lipped channel and Z-sections are commonly used due to their high strength-to-weight ratio, economy of transportation and handling, ease of fabrication, simple erection and installation. Figure 1(b) shows the use of lipped channel beams (LCB) in floor systems with circular web openings.



(a) LCB with Web Openings



(b) LCB Application

Figure 1: LCBs with Web Openings

Generally flooring systems include openings in the web of floor joists or bearers so that building services can be located within LCBs (Figure 1 (b)). Although various shapes can be used for these web openings, the most common shape is circular. The investigation of cold-formed steel sections containing web openings was undertaken in the last decade. However, only limited research has been undertaken on the effect of web openings in relation to LCB with web openings (Schuster, 1995), Shan et al., 1997 and Eiler, 1997). Shan et al. (1997) recommended that the nominal shear capacity of cold-formed lipped channel beams with web openings can be calculated using a reduction factor (q_s) applied to the solid web strength of the shear element. Eiler (1997) extended Shan et al.'s (1997) work to include the behaviour of web elements with openings subjected to linearly varying shear force. In Eiler's tests, cold-formed steel beams with web openings were subjected to a uniform load (not constant shear). Eiler (1997) also proposed suitable design equations for the shear strength of cold-formed steel beams with web openings. These equations have been adopted in AISI (2007) and AS/NZS 4600 (SA, 2005).

The use of web openings in a beam section significantly reduces its shear capacity due to the reduced web area. There are many variables that affect the

shear capacity of members containing web openings. They include the shape, size and location of the web openings and also the slenderness of the web element. This research investigated the effect of circular web openings of varying diameters on the shear capacities of LCB sections using finite element analyses (FEA) and experimental study. The LCB shear capacities were compared with the predicted shear capacities using the current design rules in AS/NZS 4600 (SA, 2005) and the North American Specification (AISI, 2007). This paper presents the details of the numerical study into the shear behaviour and design of LCBs with web openings, and the results.

2. Shear Capacity of LCBs without Web Openings

Pham and Hancock (2010) performed both experimental and numerical studies to investigate the shear behaviour of high strength cold-formed steel channel sections. From these studies they proposed suitable design equations for the shear capacity of channel sections (Equations (1) to (3)). These equations predict the shear strength of lipped channel beams, which include the available post-buckling strength in LCBs and the effect of additional fixity at the web-flange juncture (Pham, 2010). In these equations the Direct Strength Method based nominal shear capacity (V_v) is proposed using the local buckling (M_{sl}) equation where M_{sl} , M_{ol} and M_y are replaced by V_v , V_{cr} (elastic buckling capacity in shear) and V_y (shear yield capacity), respectively.

$$V_v = \left[1 - 0.15 \left(\frac{V_{cr}}{V_y} \right)^{0.4} \right] \left(\frac{V_{cr}}{V_y} \right)^{0.4} V_y \quad (1)$$

$$V_y = 0.6 A_w f_{yw} \quad (2)$$

$$V_{cr} = \frac{k_v \pi^2 E A_w}{12(1-\nu^2) \left(\frac{d_1}{t_w} \right)^2} \quad (3)$$

where k_v is the elastic shear buckling coefficient of LCB (Pham, 2010).

Keerthan and Mahendran (2011) proposed suitable shear strength equations for the new hollow flange channel sections known as LiteSteel beams (LSB) based on the current shear strength design equations in AISI (2007), experimental and finite element analysis results. They also extended this research work on shear to LCBs subjected to primarily shear action. Equations (4) to (6) present the proposed shear strength equations which include the available post-buckling strength in LCBs and the additional fixity at the web-flange juncture. The shear capacity in kN can be obtained by multiplying the shear strength (τ_v) by its

web area of $d_1 t_w$. The increased shear buckling coefficient given by Equation 7 (k_{LCB}) is included to allow for the additional fixity in the web-flange juncture of LCBs (Keerthan and Mahendran, 2011).

$$\tau_v = \tau_{yw} \quad \text{for} \quad \frac{d_1}{t_w} \leq \sqrt{\frac{Ek_{LCB}}{f_{yw}}} \quad (4)$$

$$\tau_v = \tau_i + 0.2(\tau_{yw} - \tau_i) \quad \text{for} \quad \sqrt{\frac{Ek_{LCB}}{f_{yw}}} < \frac{d_1}{t_w} \leq 1.508 \sqrt{\frac{Ek_{LCB}}{f_{yw}}} \quad (5)$$

$$\tau_v = \tau_e + 0.2(\tau_{yw} - \tau_e) \quad \text{for} \quad \frac{d_1}{t_w} > 1.508 \sqrt{\frac{Ek_{LCB}}{f_{yw}}}$$

(6)

$$\text{where} \quad \tau_i = 0.6 f_{yw} \quad \tau_i = \frac{0.6 \sqrt{Ek_{LCB} f_{yw}}}{\left[\frac{d_1}{t_w} \right]} \quad \tau_e = \frac{0.905 Ek_{LCB}}{\left[\frac{d_1}{t_w} \right]^2}$$

$$\text{For LCBs} \quad k_{LCB} = k_{ss} + 0.23(k_{sf} - k_{ss}) \quad (7)$$

$$k_{ss} = 5.34 + \frac{4}{(a/d_1)^2} \quad \text{for} \quad \frac{a}{d_1} \geq 1 \quad (8)$$

$$k_{sf} = 8.98 + \frac{5.61}{(a/d_1)^2} - \frac{1.99}{(a/d_1)^3} \quad \text{for} \quad \frac{a}{d_1} \geq 1 \quad (9)$$

where k_{ss} , k_{sf} = shear buckling coefficients of plates with simple-simple and simple-fixed boundary conditions. a = shear span of web, d_1 = clear height of web, f_{yw} = web yield stress.

3. Experimental Studies

Thirty two shear tests (Table 1) were conducted to investigate the shear behaviour of LCBs with web openings. Several important issues were considered when deciding the parameters such as the ratios of the depth of web openings to clear height of web (d_{wh}/d_1) and the clear height of web to thickness of web (d_1/t_w). In this study, test specimens of LCBs with circular web openings were designed to fail in shear prior to reaching other section capacities.

Table 1: Comparison of Ultimate Shear Capacities of LCBs from FEA and Tests

No.	LCB Section	Aspect Ratio	t_w (mm)	d_1 (mm)	f_{yw} (MPa)	d_{wh} (mm)	d_{wb}/d_1	V_v (kN)		Test/FEA
								Test	FEA	
1	120x50x18x1.95	1.0	1.94	118.6	271	0	0.00	38.08	37.40	1.02
2	120x50x18x1.95	1.0	1.95	118.1	271	30	0.25	32.31	31.60	1.02
3	120x50x18x1.95	1.0	1.94	117.7	271	60	0.51	22.17	21.20	1.05
4	120x50x18x1.95	1.0	1.95	118.3	271	80	0.68	14.97	14.20	1.06
5	120x50x18x1.5	1.0	1.49	116.8	537	0	0.00	43.33	45.35	0.95
6	120x50x18x1.5	1.0	1.50	116.6	537	80	0.69	15.97	14.90	1.07
7	160x65x15x1.9	1.0	1.91	156.8	515	0	0.00	73.80	70.50	1.05
8	160x65x15x1.9	1.0	1.92	157.7	515	30	0.19	65.37	63.00	1.04
9	160x65x15x1.9	1.0	1.90	157.5	515	60	0.38	49.53	47.00	1.05
10	160x65x15x1.9	1.0	1.91	157.6	515	100	0.63	27.61	25.80	1.07
11	160x65x15x1.9	1.0	1.90	157.3	515	125	0.79	16.88	16.10	1.05
12	200x75x15x1.9	1.0	1.91	197.0	515	0	0.00	75.80	80.50	0.94
13	200x75x15x1.9	1.0	1.90	197.0	515	30	0.15	74.83	76.00	0.98
14	200x75x15x1.9	1.0	1.91	197.0	515	60	0.30	63.35	61.00	1.04
15	200x75x15x1.9	1.0	1.90	198.0	515	100	0.51	38.83	38.70	1.00
16	200x75x15x1.9	1.0	1.90	197.5	515	125	0.63	29.38	27.50	1.07
17	120x50x18x1.95	1.5	1.95	117.0	271	0	0.00	37.30	37.30	1.00
18	120x50x18x1.95	1.5	1.94	118.0	271	60	0.51	20.28	19.35	1.05
19	120x50x18x1.95	1.5	1.94	118.0	271	80	0.68	14.22	13.50	1.05
20	120x50x18x1.95	1.5	1.95	116.0	271	100	0.86	8.27	7.70	1.08
21	120x50x18x1.9	1.5	1.90	117.0	515	0	0.00	62.80	62.80	1.00
22	120x50x18x1.9	1.5	1.91	117.5	515	60	0.51	30.01	29.40	1.02
23	120x50x18x1.9	1.5	1.90	117.8	515	80	0.68	17.14	18.15	0.94
24	120x50x18x1.9	1.5	1.90	117.5	515	100	0.85	11.45	10.85	1.06
25	160x65x15x1.5	1.5	1.50	156.4	537	0	0.00	39.70	38.10	1.04
26	160x65x15x1.5	1.5	1.49	156.4	537	100	0.64	17.39	17.50	0.99
27	160x65x15x1.5	1.5	1.51	156.0	537	125	0.80	10.18	9.80	1.04
28	200x75x15x1.9	1.5	1.90	197.0	515	0	0.00	63.36	63.40	1.00
29	200x75x15x1.9	1.5	1.90	196.8	515	30	0.15	57.09	57.00	1.00
30	200x75x15x1.9	1.5	1.91	197.2	515	60	0.30	53.09	54.50	0.97
31	200x75x15x1.9	1.5	1.89	197.0	515	100	0.51	37.15	36.50	1.02
32	200x75x15x1.9	1.5	1.90	196.9	515	125	0.63	28.82	27.50	1.05

The LCB specimens were tested using the experimental set-up shown in Figure 2. Two LCB sections were bolted back to back using three T-shaped stiffeners and web side plates located at the end supports and the loading point in order to eliminate any torsional loading of test beams and possible web crippling of flanges and flange bearing failures. In order to simulate a primarily shear condition, relatively short test beams with spans based on two aspect ratios (shear span a / clear web height d_1) of 1.0 and 1.5 were selected. A 30 mm gap was included between the two LCB sections (Figure 2) to allow the test beams to behave independently while remaining together to resist torsional effects.

High strength steel bolts were used to avoid bolt failure during testing. Flanges were restrained by straps to eliminate flange distortion due to distortional

buckling or unbalanced shear flow. The support system included pinned supports at each end. Two laser displacement transducers were located on the test beam under the loading point and web panel to measure the vertical and lateral deflections, respectively (Figure 2). Table 1 shows the lipped channel beam specimens tested in this experimental study.

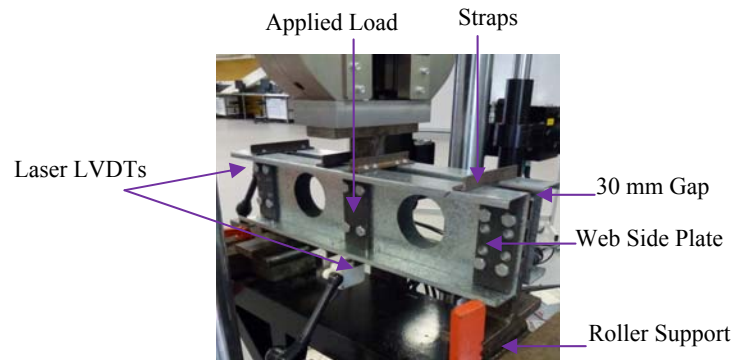


Figure 2: Experimental set-up

4. Finite Element Modelling

4.1. General

This section describes the finite element models used to investigate the shear strength and behaviour of LCB with web openings. For this purpose, a finite element program, ABAQUS Version 6.7 (HKS, 2007) was used. Appropriate parameters were chosen for the geometry, mechanical properties, loading and support conditions. Finite element models of single LCBs with shear centre loading and simply supported boundary conditions were used to simulate the 32 shear tests of back to back LCB with web openings under a three-point loading arrangement as shown in Figure 2. The cross-section geometry of the finite element model was based on the measured dimensions and yield stresses of 32 tested LCBs. Table 1 gives the measured dimensions and yield stresses of the test specimens. In this table t_w and d_l are the base metal thickness and the clear web height and f_{yw} is the web yield stress. The two methods of analysis used were bifurcation buckling and non-linear static analysis. Bifurcation buckling analyses were used to obtain the eigenvectors for the inclusion of geometric imperfections. Non-linear static analyses, including the effects of large deformation and material yielding, were employed to investigate shear strength and behaviour of LCB with web openings up to failure.

4.2. Finite Element Mesh

Shell elements were used to simulate the behaviour of the thin-walled LCB sections. The element defined as S4R5 in ABAQUS was selected for all the finite element models. The S4R5 element is a thin, shear flexible, isoparametric quadrilateral shell with four nodes and five degrees of freedom per node, and utilises reduced integration and bilinear interpolation schemes. R3D4 rigid body elements were used to simulate the restraints and loading in the finite element models of LCB with web openings. Convergence studies showed that an element size of 5 mm x 5 mm provided an accurate representation for the shear behaviour of LCBs with web openings. In order to get accurate results, Paver Mesh was applied around the web openings. The geometry and finite element mesh of a typical LCB with web openings is shown in Figure 3.

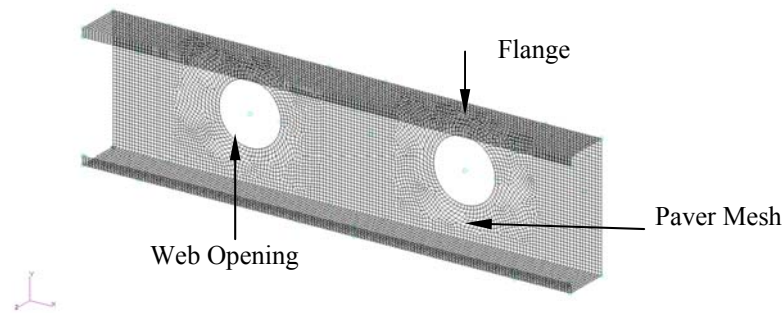


Figure 3: Geometry and Finite Element Mesh of LCBs with Web Openings

4.3. Material Model and Properties

The ABAQUS classical metal plasticity model was used for all the analyses. This model implements the von Mises yield surface to define isotropic yielding, associated plastic flow theory, and either perfect plasticity or isotropic hardening behaviour. A perfect plasticity model was adopted for all the finite element models. Measured yield stresses were used in the analyses. The elastic modulus and Poisson's ratio were taken as 200,000 MPa and 0.3, respectively.

4.4. Loads and Boundary Conditions

Simply supported boundary conditions were implemented in the finite element models of LCBs with web openings.

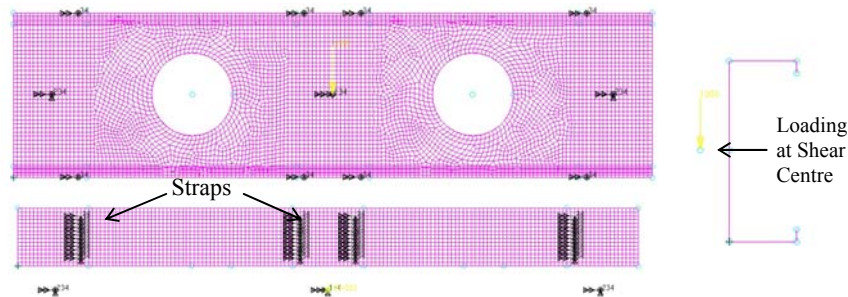
Left and right supports: $u_x = 0$ $u_y = 1$ $u_z = 1$ $\theta_x = 1$ $\theta_y = 0$ $\theta_z = 0$

Mid-span loading point: $u_x = 1$ $u_y = 0$ $u_z = 1$ $\theta_x = 1$ $\theta_y = 0$ $\theta_z = 0$

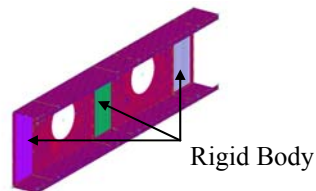
Experimental studies showed that strap failures did not occur. Considering this observation, the straps were not explicitly modelled. Instead they were simulated using suitable boundary conditions as follows.

Strap Locations: $u_x = 0$ $u_y = 0$ $u_z = 1$ $\theta_x = 1$ $\theta_y = 0$ $\theta_z = 0$

In the above, u_x , u_y and u_z are translations and θ_x , θ_y and θ_z are rotations in the x , y and z directions, respectively, and 0 denotes free and 1 denotes restrained. The vertical translation was not restrained at the loading point. Figure 4 shows the applied loads and boundary conditions of the model. Single point constraints and concentrated nodal forces were used in the finite element models to simulate the experimental boundary conditions. In order to prevent twisting, the applied point load and simply supported boundary conditions were applied at the shear centre using the rigid body reference node. Shear test specimens included a 75 mm wide plate at each support to prevent lateral movement and twisting of the cross-section. These stiffening plates were modelled as rigid bodies using R3D4 elements. Simply supported boundary conditions were applied to the rigid body reference node at the shear centre in order to provide an ideal pinned support.



(a) Loads and Boundary Conditions



(b) Rigid Body

Figure 4: Application of Loads and Boundary Conditions to LCBs

4.5. Initial Geometric Imperfections and Residual Stresses

The magnitude of local imperfections was taken as $0.006d_1$ for all the LCB sections (Schafer and Pekoz, 1998). The critical imperfection shape was introduced using the *IMPERFECTION option in ABAQUS. Preliminary finite element analyses showed that the effect of residual stresses on the shear capacity of LSBs without openings is less than 1% (Keerthan and Mahendran, 2011). Therefore the effect of residual stresses on the shear capacity of LCBs with web openings is also likely to be very small. It was thus decided to neglect the residual stresses in the FEA of LCBs with web openings.

5. Validation of Finite Element Model

It is necessary to validate the developed finite element models for non-linear analyses of LCBs with web openings subjected to shear. Thirty two models were developed using the measured material and geometric properties in experiments. Table 1 presents a summary of the FEA results of applied load and a comparison of these results with the corresponding experimental results. The mean and COV of the ratio of test to FEA applied loads are 1.02 and 0.036. This indicates that the finite element models developed in this study are able to predict the ultimate shear capacity of LCBs. Figure 5 shows the FEA results in the form of applied load versus deflection for 160x65x1.9 LCB with 60 mm web openings (Test Specimen 9) and compares them with corresponding experimental results while Figure 6 shows the shear failure modes of 200x75x1.9 LCB with 125 mm web openings (Test Specimen 32). These figures demonstrate a good agreement between the results from FEA and experiments and confirm the adequacy of the developed finite element models in predicting the ultimate loads, deflections and failure modes.

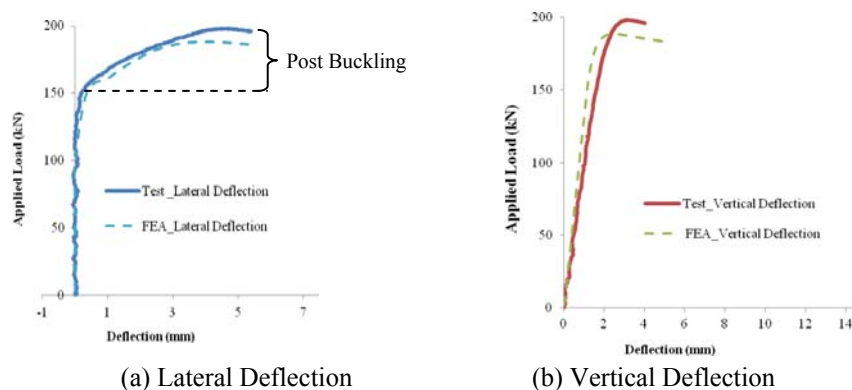


Figure 5: Plot of Applied Load versus Deflections for Test Specimen 9

Figure 5(a) shows that initially the web began to deflect out of plane (applied load of 145 kN/4) and reached the ultimate shear capacity of 49.5 kN (applied load of 198 kN/4). This confirms that LCBs with web openings have post-buckling strength due to the presence of tension field action. Figure 6 (c) shows that the tension field action observed in the shear tests was also predicted by FEA. It also confirms that simply supported conditions are sufficient to develop the post-buckling strength of LCBs due to the presence of tension field action.

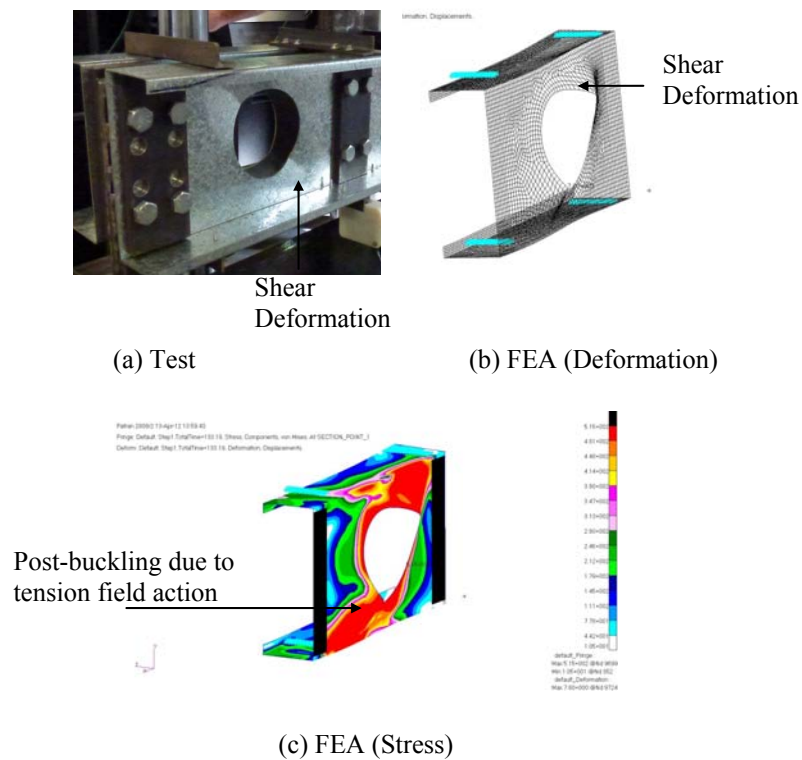


Figure 6: Failure Mode of 200x75x15x1.9 LCB with 125 mm Web Openings (Aspect Ratio = 1.5)

6. Parametric Study and Proposed Equations

A detailed parametric study was undertaken based on the validated finite element model to develop an extensive shear strength data base. In this study an aspect ratio of 1.0 was used. Five LCB sections, 120x50x18x1.95 LCB,

160x65x15x1.9 LCB, 200x75x1.0 LCB, 200x75x1.5 LCB and 200x75x15x1.9 LCB were selected in the parametric study and some of the ultimate shear capacities of LCBs with web openings for varying ratios of d_{wh}/d_1 are given in Table 2.

Table 2: Shear Capacity Reduction Factor (q_s) of LCBs with Web Openings

No.	LCB Section	d_1 (mm)	t_w (mm)	f_v (MPa)	d_{wh} (mm)	d_{wh}/d_1	V_v (kN)	q_s
1	200x75x15x1.9	200	1.9	500	0	0.00	75.50	1.00
2	200x75x15x1.9	200	1.9	500	30	0.15	75.50	0.95
3	200x75x15x1.9	200	1.9	500	60	0.30	75.50	0.78
4	200x75x15x1.9	200	1.9	500	100	0.50	75.50	0.49
5	200x75x15x1.9	200	1.9	500	125	0.63	75.50	0.35
6	200x75x15x1.5	200	1.5	500	0	0.00	52.50	1.00
7	200x75x15x1.5	200	1.5	500	30	0.15	52.50	0.95
8	200x75x15x1.5	200	1.5	500	100	0.50	52.50	0.55
9	200x75x15x1.5	200	1.5	500	125	0.63	52.50	0.33
10	200x75x15x1.0	200	1.0	500	0	0.00	26.55	1.00
11	200x75x15x1.0	200	1.0	500	30	0.15	26.55	0.98
12	200x75x15x1.0	200	1.0	500	100	0.50	26.55	0.55
13	200x75x15x1.0	200	1.0	500	125	0.63	26.55	0.37
14	200x75x15x1.5	200	1.5	300	0	0.00	35.90	1.00
15	200x75x15x1.5	200	1.5	300	30	0.15	35.90	0.94
16	200x75x15x1.5	200	1.5	300	100	0.50	35.90	0.54
17	200x75x15x1.5	200	1.5	300	125	0.63	35.90	0.34
18	200x75x15x1.0	200	1.0	300	0	0.00	19.20	1.00
19	200x75x15x1.0	200	1.0	300	30	0.15	19.20	0.95
20	200x75x15x1.0	200	1.0	300	100	0.50	19.20	0.52
21	200x75x15x1.0	200	1.0	300	125	0.63	19.20	0.34

The currently available shear capacity reduction factor equations were used to predict the shear capacities of the tested and analysed LCB sections. However, they were found to be either conservative or unsafe when compared with FEA and experimental shear capacities. Therefore new equations are proposed to predict the shear capacity of LCBs with web openings based on FEA and experimental results. It is proposed that the shear capacity of LCBs with web openings (V_{nl}) can be calculated using a reduction factor q_s applied to the shear capacity of LCBs without web openings (V_v). The use of a shear capacity

reduction factor (q_s) to the shear capacities of LCBs without web openings is considered adequate as a simple design method. Section 2 presents the shear capacity equations for LCBs without web openings (V_v) as Eqs. (1) to (6). Equations 10 to 13 show the proposed design equations for the shear capacity of LCBs with web openings (V_{nl}).

$$V_{nl} = q_s V_v \quad d_{wh} / d_1 \leq 0.85 \quad (10)$$

$$q_s = 1 - 0.6 \left[\frac{d_{wh}}{d_1} \right] \quad 0 < \frac{d_{wh}}{d_1} \leq 0.30 \quad (11)$$

$$q_s = 1.215 - 1.316 \left[\frac{d_{wh}}{d_1} \right] \quad 0.30 < \frac{d_{wh}}{d_1} \leq 0.70 \quad (12)$$

$$q_s = 0.732 - 0.625 \left[\frac{d_{wh}}{d_1} \right] \quad 0.70 < \frac{d_{wh}}{d_1} \leq 0.85 \quad (13)$$

q_s = shear capacity reduction factor = V_{nl}/V_v , d_{wh} = depth of web openings
 d_1 = clear height of web

In order to investigate the effect of web yield stress (f_{yw}) and clear height of web to web thickness ratio (d_1/t_w) on the ultimate shear capacity of LCBs with web openings, the same FE model was used with varying web thickness (t_w) and web yield stress (f_{yw}) values. The clear web height to thickness ratio (d_1/t_w) was varied by simply changing the web thickness. Table 2 indicates that the web yield stress (f_{yw}) and the clear height of web to web thickness ratio (d_1/t_w) have only a small effect on the ultimate shear capacity of LCBs with web openings (shear capacity reduction factor (q_s) did not vary much with f_{yw} and d_1/t_w).

Figure 7 shows the non-dimensional curve of q_s versus d_{wh}/d_1 . In order to assess the accuracy of the proposed design equations for the shear capacity of LCBs with web openings (Eqs. 11 to 13), their predictions are compared with the FEA and experimental shear capacity reduction factors in Figure 7. It shows that the shear capacity reduction factors predicted by Equations 11 to 13 agree well with the FEA and experimental shear capacity reduction factors. The mean value of FEA to predicted shear capacity reduction factor ratio is 1.01 while the corresponding coefficient of variation (COV) is 0.089.

Figure 8 shows the shear capacity reduction factors of 160x65x15x1.9 LCB (aspect ratio = 1.0) as a function of depth of web opening to clear height of web

ratio in comparison to those proposed by other researchers in the past. They show that Shan et al.'s (1997) equations are very conservative for the shear capacity of LCBs with web openings. The AS/NZS 4600 (SA, 2005) design equations are conservative for LCB sections with small web openings while they are unconservative for LCB sections with large openings. However, the proposed design equations are able to accurately predict the FEA and experimental shear capacities of LCBs with web openings.

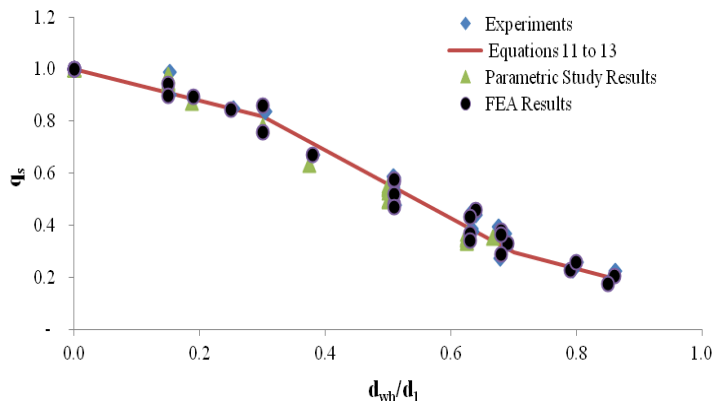


Figure 7: Shear Capacity Reduction Factor q_s versus d_{wh}/d_1 for LCBs with Web Openings

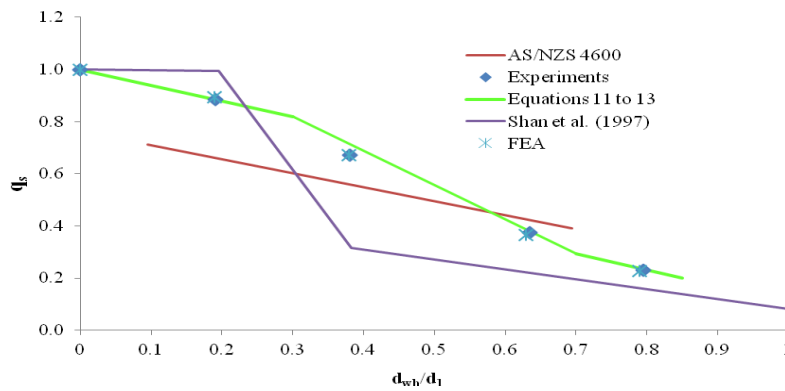


Figure 8: Shear Capacity Reduction Factor q_s versus d_{wh}/d_1 for 160x65x15x1.9 LCB (Aspect Ratio =1.0)

7. Conclusions

This paper has presented a detailed investigation into the shear strength and behaviour of lipped channel beams with web openings using finite element analyses. Suitable finite element models were developed and validated by comparing their results with corresponding test results. The developed nonlinear finite element model was able to predict the shear capacities of LCBs with web openings and associated deformations and failure modes with very good accuracy. Experimental and numerical studies show that AS/NZS 4600 (SA, 2005) design equations are conservative for LCB sections with small web openings while they are unconservative for LCB sections with large openings. It was found that Shan et al.'s (1997) design equations are too conservative for the shear capacity of LCBs with web openings. Appropriate improvements have been proposed in the form of modified shear capacity reduction factors to determine the shear capacity of LCBs with web openings based on finite element analysis and experimental results.

Acknowledgements

The authors would like to thank Australian Research Council for their financial support, and the Queensland University of Technology for providing the necessary facilities and support to conduct this research project. They would also like to thank Mr. Scott Henderson and Mr. Christopher Stevens for their valuable assistance in performing the shear tests.

References

- American Iron and Steel Institute (AISI) (2007), North American Specification for the Design of Cold-formed Steel Structural Members, AISI, Washington DC, USA.
- Eiler, M.R. (1997), Behaviour of Web Elements with Openings Subjected to Linearly Varying Shear, Masters Thesis, University of Missouri-Rolla, Missouri-Rolla, USA.
- Hibbitt, Karlsson and Sorensen, Inc. (HKS) (2007), ABAQUS User's Manual, New York, USA.

Keerthan, P. and Mahendran, M. (2011), New Design Rules for the Shear Strength of LiteSteel Beams, *Journal of Constructional Steel Research*, Vol. 67, pp. 1050–1063.

Pham, C.H. (2010), Direct Strength Method (DSM) of Design of Cold-formed Sections in Shear and Combined Bending and Shear, PhD Thesis, University of Sydney, Australia.

Pham, C.H., Hancock, G.J. (2010), Numerical Simulation of High Strength Cold-formed Purlins in Combined Bending & Shear, *Journal of Constructional Steel Research*, Vol.66, pp.1205-1217.

Schafer, B.W. and Pekoz, T. (1998), Computational Modeling of Cold-formed Steel: Characterizing Geometric Imperfections and Residual Stresses, *Journal of Constructional Steel Research* Vol 47, pp. 193-210.

Schuster, R. M. (1995), Research into Cold Formed Steel Perforated C-Sections in Shear, Progress Report No.1 of Phase I of CSSBI / IRAP Project, University of Waterloo, Waterloo, Ontario Canada.

Shan, M.Y., LaBoube, R.A., Langan, J.E. and Yu, W.W. (1997), Cold-formed Steel Webs with Openings: Summary report, *Thin-Walled Structures*, Vol. 27, pp. 79 – 84.

Standards Australia/Standards New Zealand (SA) (2005), *Australia/New Zealand Standard AS/NZS4600 Cold-Formed Steel Structures*, Sydney, Australia.